

# SCSV<sup>2</sup>: Physics-informed Self-Configuration Sensing through Vision and Vibration Context Modeling

Lixing He  
helixing99@gmail.com  
Univ. of Electronic Science  
and Technology of China  
Chengdu, China

Carlos Ruiz  
carlos@aifi.io  
AiFi Inc.  
Santa Clara, CA, USA

Mostafa Mirshekari  
mmirshek@stanford.edu  
Stanford University  
Stanford, CA, USA

Shijia Pan  
span24@ucmerced.edu  
University of California  
Merced  
Merced, CA, USA

## ABSTRACT

Structural vibration sensing has been explored to acquire indoor human information. This non-intrusive sensing modality enables various smart building applications such as long-term in-home elderly monitoring, ubiquitous gait analysis, etc. However, for applications that utilize multiple sensors to collaboratively infer this information (e.g., localization, activities of daily living recognition), the system configuration requires the location of the anchor sensor, which are usually acquired manually. This labor-intensive manual system configuration limited the scalability of the system.

In this paper, we propose SCSV<sup>2</sup>, a self-configuration scheme to compute these vibration sensor locations utilizing shared context information acquired from complementary sensing modalities – vibration sensor itself and co-located cameras. SCSV<sup>2</sup> combines 1) the physics models of wave propagation together with structural element effects and 2) the data-driven model from the multimodal data to infer the vibration sensor’s location. We conducted real-world experiments to verify our proposed method and achieved an up to 7cm anchor sensor localization accuracy.

## KEYWORDS

System self-configuration, physics-informed, heterogeneous sensing, structural vibration, computer vision, sensor localization estimation.

### ACM Reference Format:

Lixing He, Carlos Ruiz, Mostafa Mirshekari, and Shijia Pan. 2020. SCSV<sup>2</sup>: Physics-informed Self-Configuration Sensing through Vision and Vibration Context Modeling. In *Adjunct Proceedings of the 2020 ACM International Joint Conference on Pervasive and Ubiquitous Computing and Proceedings of the 2020 ACM International Symposium on Wearable Computers (UbiComp/ISWC ’20 Adjunct)*, September 12–16, 2020, Virtual Event, Mexico. ACM, New York, NY, USA, 6 pages. <https://doi.org/10.1145/3410530.3414586>

## 1 INTRODUCTION

Structural vibration-based human information inference allows non-intrusive fine-grained in-home occupant information acquisition such as identity [11], location [7], gait parameters [1], activity

Permission to make digital or hard copies of all or part of this work for personal or classroom use is granted without fee provided that copies are not made or distributed for profit or commercial advantage and that copies bear this notice and the full citation on the first page. Copyrights for components of this work owned by others than ACM must be honored. Abstracting with credit is permitted. To copy otherwise, or republish, to post on servers or to redistribute to lists, requires prior specific permission and/or a fee. Request permissions from [permissions@acm.org](mailto:permissions@acm.org).

*UbiComp/ISWC ’20 Adjunct, September 12–16, 2020, Virtual Event, Mexico*

© 2020 Association for Computing Machinery.

ACM ISBN 978-1-4503-8076-8/20/09...\$15.00

<https://doi.org/10.1145/3410530.3414586>

[9]. This occupant information enables various intelligent applications, such as elderly care, in-home patient care, etc. Many of these systems rely on multiple sensors to collaboratively infer the target information, such as multi-lateration based localization [1, 7]. The assumption for these collaboratively functioning systems often includes given locations of the anchor sensors, which are often manually notated. However, manually configure sensor locations for every deployment is inconvenient and impractical for large scale deployment. Furthermore, for sensors that can be moved around, re-configuring sensor location every time for sensor re-location is impractical especially for in-home usage. Other than manually configuring sensor locations, prior methods to acquire sensor locations mainly fall in two categories: 1) direct measuring of the sensor position [5, 6], which relies on known locations of certain anchor devices which may not always be available; 2) inferring relative location through shared context [10], which does not provide sufficient accuracy.

We present SCSV<sup>2</sup>, an active self-configuring multi-modal sensing system, which leverages the ambient information acquired from cameras and the vibration sensing signals to determine the location configuration of the vibration sensors. The intuition is that vibration sensors capture the footstep induced vibration and the camera captures the footstep physical locations<sup>1</sup>, which observes the shared context information – footstep location. Then based on the *signal energy profile* of the footstep induced signals at different locations, we derive the location of the vibration sensor.

SCSV<sup>2</sup> first analyzes the footstep signal energy change and identifies if the footfall is on a structural element, such as a beam or structural partition. Then the system associates the physical model of vibration attenuation to the structural elements inferred from the footstep induced vibration signals. Next, the system conducts a grid search on possible sensor locations and calculates the theoretical footstep energy profile for each possible sensor locations. Finally, the system matches the theoretical profiles to the observed profile and consider the corresponding sensor locations as the estimated sensor location. The contributions of this paper include

- We propose a self-configuring sensing system that utilizes data acquired from ambient environments to infer system configuration.
- We present a physics-informed algorithm utilizing complementary context information from multiple sensing modalities to profile analytical model of the sensing environment and sensing system configuration.

<sup>1</sup>Note that the camera can be removed after the bootstrap phase to considering the user privacy.

- We evaluate our system through real-world experiments.

The rest of the paper is organized as follows. First, we introduce the physics model of the structural element effects on vibration signals in Section 2. Next, we present the details of the self-calibrating scheme in Section 3. Then, we demonstrate the system performance through real-world experiments in Section 4. Finally, we present related work in Section 5 and conclude this work in Section 6.

## 2 BACKGROUND AND PHYSICAL MODEL

In real-world deployments, the wave propagation will be impacted by various structural elements and does not show an ideal attenuation pattern. To achieve accurate modeling for sensor location inference, we first introduce the model for wave propagation with supported beams. Figure 1 shows the structural model with supported beams on both ends, where we assume that people step along the floor slab between the beams. Note that in this work we focus on the 1-D analysis along the hallway, and we will further discuss the method extended to 2-D in Section 6. In a 1-D analysis, we simplify the model as a simply-supported beam with point load for footsteps for which the displacements are calculated as [2]:

$$f_{disp}(x_s, x_f, L) = \frac{-F(L - x_f)x_s}{6EI} * (L^2 - (L - x_f)^2 - x_s^2) \quad (1)$$

where  $x_f \geq x_s \geq 0$ . In Eq. 1,  $f_{disp}(x_s, x_f, L)$  denotes the beam deflection as a function of the location of the force (i.e., footstep),  $x_s$  is the distance to  $beam_1$ ,  $x_f$  is the distance between the force and  $beam_1$ ,  $L$  is the length of the floor slab between the two beams, and  $F$  represents the force of the footstep. Finally,  $E$  and  $I$  are the modulus of elasticity and the moment of inertia which are properties of the structure and are considered as constants. Further, the elastic energy that is stored in the beam is proportional to the deflection to the power of two. In general, this energy can be described as  $1/2 * k * x^2$ , in which  $k$  is the stiffness and  $x$  is the deflection (similar to the potential energy in a spring) [4]. As a side note, Eq. 1 is suitable for static loads. However, as will be shown using our results, it still well represents the relationship even though footsteps are dynamic. With the aforementioned model, we calculate the theoretical values for structural vibration signals of footsteps along the hallway (different  $x_f$  values) for sensors at different locations (different  $x_s$  values). For example, given sensor location  $x_s$ , The blue curve in Figure 1 shows the estimated relative signal energy for a consistent footstep excitation applied at different locations along the hallway, where the x-axis is the footstep location, and the y-axis is the relative signal energy.

## 3 SELF-CONFIGURATION SYSTEM ARCHITECTURE

We present our system *SCSV*<sup>2</sup>, which takes into account measurable structural elements' impact on the vibration signal to infer the sensor location from ambient sensing signals. The structural characteristics and elements (e.g., beams) directly impact the vibration propagation, and they are very commonly seen in many structures. As a result, the assumption for native method [10], which is the closer the excitation and the sensor, the higher the signal energy, will be no longer valid. *SCSV*<sup>2</sup> first utilizes the camera to acquire each footstep's location in the real-world. Then, *SCSV*<sup>2</sup> associates

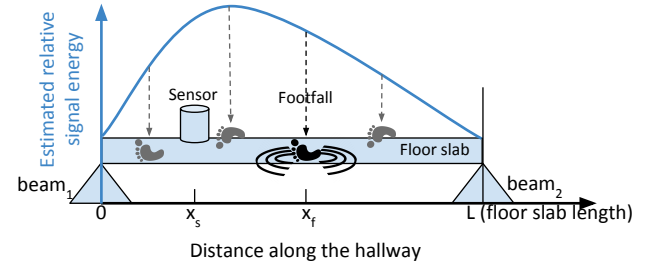


**Figure 1: Wave propagation model with beams.** The x-axis is the distance along the hallway measured from  $beam_1$ .  $x_s$  is the sensor location,  $x_f$  is the investigated footfall location,  $L$  is the floor slab length, i.e., the distance between two consecutive beams. Based on the wave propagation model described in Eq. 1, we can estimate the relative signal energy for each footfall location as shown in the blue curve.

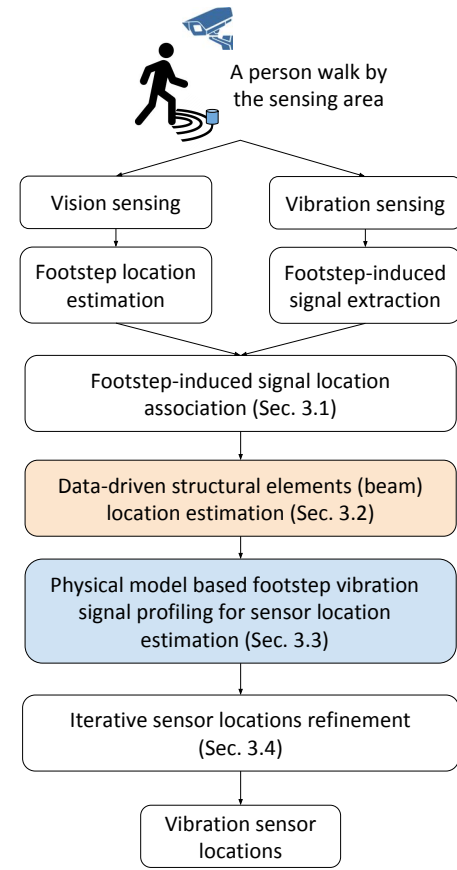


**Figure 2: System overview.**

the detected footstep-induced vibration signal to these acquired locations. The impulsive signal's characteristics can be used to infer the abnormality of the structural wave propagation, which indicates the structural elements [8]. For example, due to the high

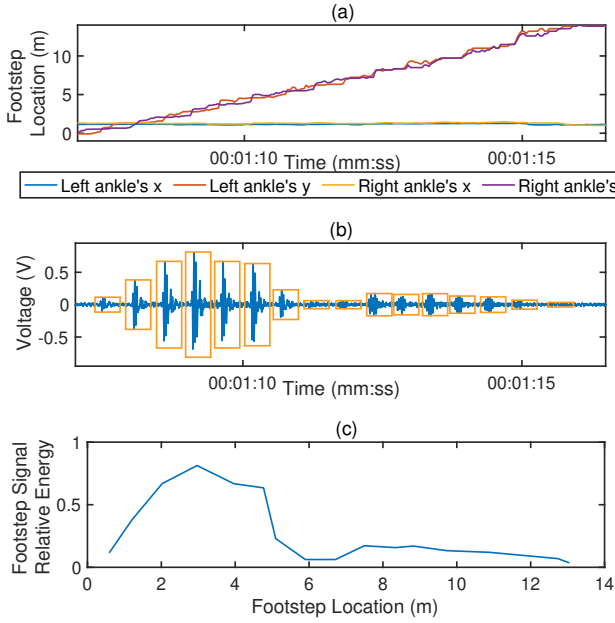


**Figure 3: Location information acquired by camera and structural vibration signals captured by geophone sensors placed at different location.**

stiffness of the beam area, the footstep on the beam will induce significantly lower vibration, and this change can be captured by our algorithm to determine the beam location. Once  $SCSV^2$  determines the beam location, it can further infer the propagation model with beam effects, which is used for sensor location estimation with the observed signal propagation properties.  $SCSV^2$  calculates the theoretical relative footstep signal energy with different possible sensor locations, as well as the observation. Then  $SCSV^2$  selects the theoretical model that shows maximum similarity to the data-driven observation and uses its sensor location as the estimated sensor location. We list the assumptions in this work as follows.

- **Assumption 1:** When a person walks by the sensing area, they maintain a consistent gait.
- **Assumption 2:** We can acquire the size of the floor slabs or the distance between structural elements (e.g., beams) from Building Information Modeling (BIM), which is marked as  $L$  in Figure 1.
- **Assumption 3:** The sensing range of the vision and vibration sensors are overlapping.
- **Assumption 4:** Footsteps are static forces.

### 3.1 Footstep-induced vibration signal location association

Localizing footsteps using footstep-induced vibration signals requires prior knowledge of the vibration sensor locations. Instead,  $SCSV^2$  utilizes other sensors in the environment –a camera– to acquire this information, then associates the vision-based footstep location estimation to the footstep-induced vibration. Thanks to recent advancements in Human Pose Estimation –a well-studied

---

#### Algorithm 1 Beam Location Estimation

---

**Input:** Footstep signal energy sequence  $f_i = [SE(x_1), \dots, SE(x_N)]$ , footstep location  $x_{1\dots N}$ ,  $N$  is the number of footstep in the trace.

**Output:** Estimated location of the beam:  $beamLoc_{est}$ .

```

function FINDBEAMLOCATION( $f_i, x_{1\dots N}$ )
    for  $stepIdx = 1 \rightarrow N$  do
         $f_{HF}(x'_{1\dots M}) \leftarrow Interpolate(f_i, x_{1\dots N})$ 
    end for
     $f_{sign}(x') \leftarrow sign(\frac{\partial(smooth(f_{HF}(x')))}{\partial x})$ 
    for  $locIdx = 1 \rightarrow M$  do
        if  $f_{sign}(x'_{locIdx})$  change from negative to positive then
             $beamLoc = x'_{locIdx}$ 
        end if
    end for
end function

```

---

problem in the Computer Vision literature that tries to estimate the location of joints and limbs of people found in images–,  $SCSV^2$  can track the pedestrian’s heels. However, one more step is needed to map the output 2D pixel coordinates to the projected position on the floor. This can be achieved by leveraging extrinsic calibration [17] (which simply requires 3 or more points on the floor plane to be determined). Note that the 2D pixel of the estimated heel location determines a 3D line where the heel lies at an unknown depth. Given the ground plane, we can determine the 3D foot location as the intersection between that line and the  $z = Z_{cm}$  plane, where  $Z$  is the expected heel height to the floor. Figure 3a shows the vision-based ankle location estimation in the x and y-axis in the sensing area. Figure 3b shows the structural vibration signal captured by a vibration sensor placed on the surface of the hallway. The blue line is the raw floor vibration signal captured by the vibration sensor, and the yellow box is the detected **footstep events**. For each detected footstep events (Figure 3b), we assign its location as the location detected by the vision sensor (Figure 3a), the result can be seen on (Figure 3c). In this work, we focus on 1-D along the hallway and define consecutive footstep events passing by the sensing area as a **trace**. We further define the series of signal energy of footstep events in the  $i^{th}$  trace as

$$f_i = [SE(x_1), \dots, SE(x_N)] \quad (2)$$

where  $N$  is the number of footsteps within the trace,  $x_j$  is the location of the  $j^{th}$  footstep event,  $j \in [1, \dots, N]$ .

### 3.2 Data-driven structural element location estimation

For an ‘ideal’ floor structural, the theoretical model for the surface wave propagation follows the  $SE(d) \propto 1/d$ , where  $SE$  is the signal energy of a footstep event, and  $d$  is the distance between the sensor and the footstep event [7]. However, for the real-world deployment as demonstrated in Figure 3b, we observe that between the time slot 01:11 and 01:12, the footstep induced vibration signal energy does not follow the simplified model. This phenomenon is caused by the beam effect as we discussed in Section 2.

We present a beam detection Algorithm 1 based on the footstep-induced floor vibration signal. The algorithm first interpolates the data points in the *signal energy profile* from one trace (Figure 3c) to achieve a higher resolution location-signal energy relation mapping, which we denote as  $f_{HR}(x'_{1\dots M})$  for the M locations after interpolation. Then  $SCSV^2$  conducts a moving average to smooth  $f_{HR}(x')$  and takes the derivative of it. Next,  $SCSV^2$  calculates the sign of the derivative as  $f_{sign}(x')$ . We identify the location  $x'$  where the  $f_{sign}(x')$  changes from negative to positive to locate the ‘valley’ of the curve, which indicates an anomaly of footstep signal energy due to the high stiffness of the structure within the area. We assign the corresponding location  $x'$  as the beam location. We assume that  $SCSV^2$  can acquire the floor slab length  $L$  from the building information modeling (BIM) and infer the nearby beam locations accordingly even the camera view may not cover the area.

### 3.3 Physical model based footstep event profiling for sensor location estimation

Once  $SCSV^2$  estimated the beam location, we can estimate the relative signal energy at a given footfall location (as shown in Figure 1  $x_f$ ) and a given sensor location (as shown in Figure 1  $x_s$ ).  $SCSV^2$  conducts a grid search for sensor location  $x_s \in (0, L)$  between two beams. For each investigated sensor location  $x_s$ ,  $SCSV^2$  calculates the estimated relative signal energy curve as shown in Figure 1 on the detected footfall location  $x_f$  as  $f_{disp}(x_s, x_f, L)$ . Then  $SCSV^2$  reports the  $x_s$  such that

$$\underset{x_s}{\operatorname{argmax}}(\operatorname{corr}(f_i, f_{disp}(x_s, x_f, L)))$$

as the estimated sensor location, where  $\operatorname{corr}$  denotes the computation of the correlation coefficient and  $f_i$  is the data-driven observation of the  $i^{th}$  trace as defined in Eq. 2.

### 3.4 Iterative sensor location refinement

Because of the uncertainty of the footfall locations as well as the measurement noise, the accuracy of the sensor location estimation varies over different traces. Since it is common that multiple occupants may pass by the sensing area, and the sensor location can be estimated every time they pass by,  $SCSV^2$  further refines the sensor location with historical estimation results. When there are less than three traces,  $sensorLoc$  is calculated as the estimated value of the first trace. Otherwise,  $SCSV^2$  calculates the mean  $\mu$  and the standard deviation  $\sigma$  of the historical data and conducts an anomaly detection to discard estimation that is out of the range  $[\mu - \sigma, \mu + \sigma]$ .  $SCSV^2$  updates the sensor location estimation as

$$sensorLoc_i = \begin{cases} a * sensorLoc_{i-1} + (1 - a) * x_s & x_s \in [\mu - \sigma, \mu + \sigma] \\ sensorLoc_{i-1} & x_s \notin [\mu - \sigma, \mu + \sigma] \end{cases} \quad (3)$$

Where  $sensorLoc_i$  denotes the estimation of sensor location at the  $i^{th}$  iteration and  $x_s$  represents the estimation from the  $i^{th}$  trace as discussed in Section 3.3. In our implementation, we set  $a = 0.5$ .

## 4 EVALUATION

To evaluate our physical model and data-driven combined automatic sensing configuration estimation method, we conducted experiments on the real-world multi-modal sensing dataset.

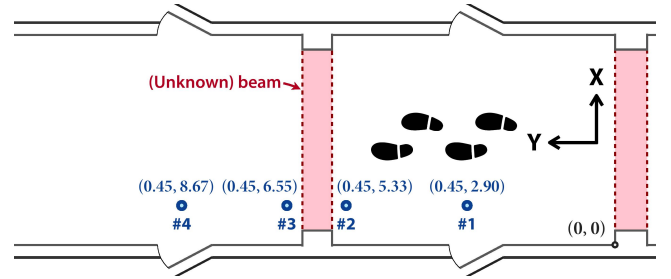


**Figure 4: Experimental setup and sensing area.** Point (0,0) is marked based on the camera view and coordinates.

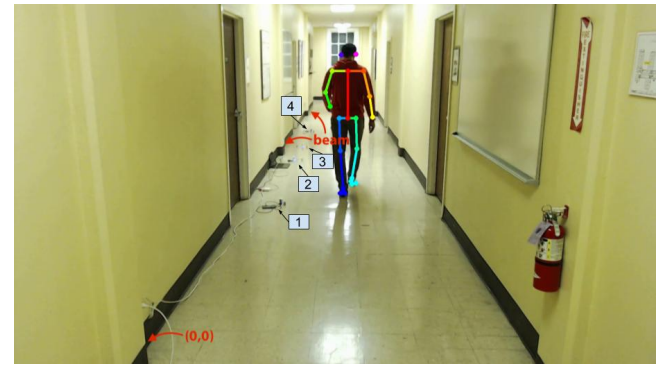


**Figure 5:** Camera view of the sensing area. The left bottom corner of the floor is the corresponding point to the (0,0) marked in Figure 4. Four sensors' locations are pointed out in the camera view with their Sensor ID.

### 4.1 Experiment setup

The dataset consists of four structural vibration sensors and one camera’s data. Figure 4 demonstrates the locations of four vibration sensors placed in a hallway with structural elements such as beams. Figure 5 shows the camera view of the corresponding sensing area shown in Figure 4. During the experiment, the participant walked back and forth between  $y=0$  and  $y=14$ . We collected 11 traces for both vision and vibration data.

### 4.2 Results and analysis

We evaluate 1) the beam location and 2) the sensor location using Mean Absolute Error (MAE). We define the metric as

$$MAE = \frac{1}{N} \|Loc_{gt} - Loc_{est}\|_1 \quad (4)$$

where  $Loc_{gt}$  is the ground truth location and  $Loc_{est}$  is the location estimated by  $SCSV^2$ .

We consider the pure data-driven approach as the **baseline**, where the location of the *signal energy profile* with the maximum signal energy is considered as the sensor location.

**Beam location estimation analysis.** The ground truth of the beam location in the camera view coordinate is 5.94m from the (0,0) point. The  $MAE_{beam}$  over 11 traces is 0.3304 meters, with a standard deviation of 0.0375. Figure 6 plots the beam location estimation error for

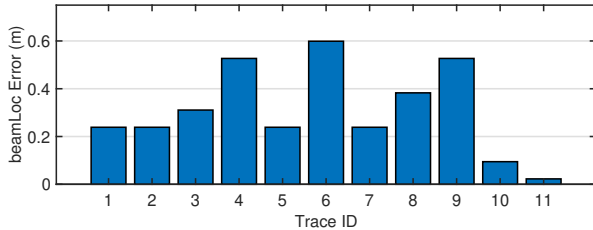


Figure 6: Results of beam location estimation.

each trace. We notice that the error rate varies over different traces, which could be caused by the variation of the footstep locations in each trace.

*Sensor location estimation analysis.* We investigate how does the number of iterations impacts the sensor location estimation. Figure 7 shows the sensor location estimation error after different numbers of iterations, where the x-axis is the iteration number and y-axis is the sensor location estimation error. For  $k$  number of iteration, we randomly select  $k$  traces with random orders and repeat 30 times. We plot the MAE for both our method and the baseline method in Figure 7, where the blue line represents our method, and the red line represents the baseline method. We observe that for the baseline method, the error is consistent over multiple iterations. Sensor 2 and 3 demonstrate a similar level of MAE with an average around 2m, while Sensor 1 and 4 demonstrate a similar level of MAE with an average around 1m. This is because of the beam effect that distorts the estimation for sensors closer to the beam more. With 11 iterations, our method achieves an average error as low as 0.36m, 1m, and 0.07m, while the baseline's average error is 0.69m, 1.48m, and 2.28m, respectively for Sensor 1, 2, and 3. For Sensor 4, our method yields an average error of 2.5m, which is caused by the high error rate of vision-based footstep location estimation due to the long distance between the target sensing area and the camera. In summary, our system achieves an **up to 7cm** sensor location estimation accuracy, corresponding to a 32.5x improvement compared to the baseline method. The improvement over four investigated sensors with varying distance to the camera shows an average of 1.39x improvement.

## 5 RELATED WORK

Various methods have been conducted to **estimate the device location**, such as acoustic-, RF-, vision-, and light-based methods [3, 12, 14, 15]. However, these methods either suffers from high error rate (i.e., 1-2.7m [12]), or require special sensor/sensing condition (microphone [14], line-of-sight [3, 15]). SCSV<sup>2</sup> does not require additional sensors nor line-of-sight for localization, instead, it inverted the vibration-based footstep localization to infer sensor locations with camera-based footstep location information, and achieved up to 7cm localization accuracy.

Recent work has been done on combining computer vision and wearable sensors through **shared context to achieve device association** to their location in the camera view [13]. However, such association relies on a directly comparable shared measurement

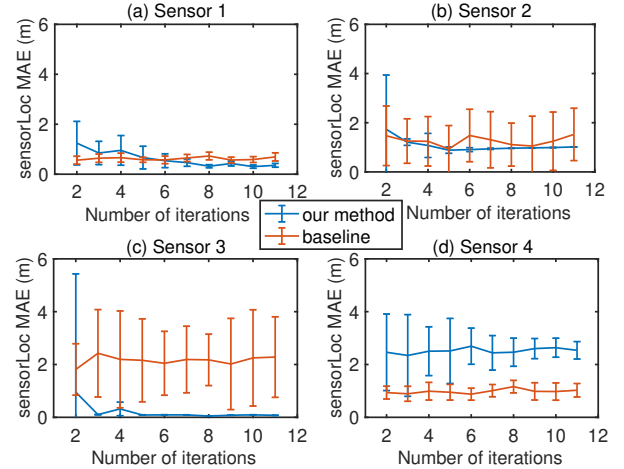


Figure 7: Results of sensor location estimation over different number of iterations.

– body part motion, which does not apply to the subtle micromotion of the floor. In this work, we combine the physics model of footstep-induced vibration signal wave propagation and structural element’s effect to augment the shared context measured by the vision and floor vibration and achieve the vibration sensor location estimation.

Besides, prior work has been done on **structural characterization through ambient vibration** sensing signal, including data-driven floor slab separation identification [8] and floor wave propagation decay model estimation [16]. However, their information inference resolution is at the floor slab level and not sufficient for sensor location estimation that can further enable sensor-location-aware applications.

## 6 DISCUSSION

We discuss the potential future directions for SCSV<sup>2</sup> in this section.

### 6.1 Model generalization and adaptation

We explored the feasibility of self-configuration systems through a set of experiments under a controlled environment. Potential factors that may impact the model is structural variation. For example, different structural elements (e.g., beams, load-bearing wall) would result in different analytical models of wave propagation. Different materials would result in different decay rates and wave propagation profiles. As a result, a more generalized framework that combines physical and data-driven models can be developed adaptively with multiple optional physics models. We plan to conduct experiments on different types of structures and configurable floors in the future to demonstrate the system and model generalizability.

### 6.2 Extend dimensions

We focus on 1-D scenario sensor location estimation in this work and we plan to extend the method for 2-D scenarios that can be applied for areas that have more dynamic pedestrian traffics (e.g., hall, mall). When pedestrians walk towards different directions, we

can utilize the method introduced in this paper to acquire the sensor location along that direction. As a result, when pedestrians pass by the sensing area in different directions, we can utilize the 2-D relation of their trajectories to achieve the automatic 2-D sensor location estimation through multimodal sensing for shared context.

### 6.3 Combine data acquisition quality for optimal deployment

The structural elements, such as beams, not only impact sensor location estimation as well as acquired data quality (e.g., signal to noise ratio) due to its structural properties. Prior work on sensing system deployment data acquisition quality assessment [16] can be combined with the physics-informed structural element detection and localization method introduced in this work to provide optimization feedback control for the deployment.

## 7 CONCLUSION

In this paper, we introduce *SCSV<sup>2</sup>*, a self-configuring structural vibration sensing system that can estimate sensor location automatically using a co-located vision sensor. A data-driven structural element location estimation algorithm and a sensor location estimation algorithm that combines physical-and-data-driven model are presented. Real-world experiments are conducted to evaluate *SCSV<sup>2</sup>*, where our system achieved up to 7cm sensor location estimation accuracy and demonstrated an average of 1.39x improvement compared to the pure data-driven baseline.

## REFERENCES

- [1] Jonathon Fagert, Mostafa Mirshekari, Shijia Pan, Pei Zhang, and Hae Young Noh. 2017. Characterizing left-right gait balance using footstep-induced structural vibrations. In *Sensors and Smart Structures Technologies for Civil, Mechanical, and Aerospace Systems 2017*, Vol. 10168. International Society for Optics and Photonics, 1016819.
- [2] Russell Charles Hibbeler and SC Fan. 2004. *Statics and mechanics of materials*. Vol. 2. Prentice Hall Upper Saddle River.
- [3] Alex Kushleyev, Daniel Mellinger, Caitlin Powers, and Vijay Kumar. 2013. Towards a swarm of agile micro quadrotors. *Autonomous Robots* 35, 4 (2013), 287–300.
- [4] Lev Davidovich Landau. 1989. *Theory of Elasticity Ed 3 Vol 7*. Pergamon press.
- [5] William Wei-Liang Li, Ronald A Iltis, and Moe Z Win. 2013. A smartphone localization algorithm using RSSI and inertial sensor measurement fusion. In *2013 IEEE Global Communications Conference (GLOBECOM)*. IEEE, 3335–3340.
- [6] Kaikai Liu, Xinxin Liu, and Xiaolin Li. 2013. Guoguo: Enabling fine-grained indoor localization via smartphone. In *Proceeding of the 11th annual international conference on Mobile systems, applications, and services*, 235–248.
- [7] Mostafa Mirshekari, Shijia Pan, Jonathon Fagert, Eve M Schooler, Pei Zhang, and Hae Young Noh. 2018. Occupant localization using footstep-induced structural vibration. *Mechanical Systems and Signal Processing* 112 (2018), 77–97.
- [8] Shijia Pan. 2018. *Indoor Human Information Acquisition from Physical Vibrations*. Ph.D. Dissertation. Carnegie Mellon University.
- [9] Shijia Pan, Mario Berges, Juleen Rodakowski, Pei Zhang, and Hae Young Noh. 2019. Fine-Grained Recognition of Activities of Daily Living through Structural Vibration and Electrical Sensing. In *Proceedings of the 6th ACM International Conference on Systems for Energy-Efficient Buildings, Cities, and Transportation*, 149–158.
- [10] Shijia Pan, Amelie Bonde, Jie Jing, Lin Zhang, Pei Zhang, and Hae Young Noh. 2014. Boes: building occupancy estimation system using sparse ambient vibration monitoring. In *Sensors and Smart Structures Technologies for Civil, Mechanical, and Aerospace Systems 2014*, Vol. 9061. International Society for Optics and Photonics, 90611O.
- [11] Shijia Pan, Tong Yu, Mostafa Mirshekari, Jonathon Fagert, Amelie Bonde, Ole J Mengshoel, Hae Young Noh, and Pei Zhang. 2017. Footprintid: Indoor pedestrian identification through ambient structural vibration sensing. *Proceedings of the ACM on Interactive, Mobile, Wearable and Ubiquitous Technologies* 1, 3 (2017), 1–31.
- [12] Neal Patwari, Alfred O Hero, Matt Perkins, Neiyer S Correal, and Robert J O’dea. 2003. Relative location estimation in wireless sensor networks. *IEEE Transactions on signal processing* 51, 8 (2003), 2137–2148.
- [13] Carlos Ruiz, Shijia Pan, Adeola Bannis, Ming-Po Chang, Hae Young Noh, and Pei Zhang. 2020. IDIoT: Towards Ubiquitous Identification of IoT Devices through Visual and Inertial Orientation Matching During Human Activity. In *2020 IEEE/ACM Fifth International Conference on Internet-of-Things Design and Implementation (IoTDI)*. IEEE, 40–52.
- [14] Zheng Sun, Auke Purohit, Kaifei Chen, Shijia Pan, Trevor Pering, and Pei Zhang. 2011. PANDAA: physical arrangement detection of networked devices through ambient-sound awareness. In *Proceedings of the 13th international conference on Ubiquitous computing*, 425–434.
- [15] Ran Zhang, Wen-De Zhong, Dehao Wu, and Kemao Qian. 2016. A novel sensor fusion based indoor visible light positioning system. In *2016 IEEE globecom workshops (GC wkshps)*. IEEE, 1–6.
- [16] Yue Zhang, Susu Xu, Laixi Shi, and Shijia Pan. 2020. Using Mobile Sensing to Enable the Signal Quality Assessment for Infrastructure Sensing Systems. In *Proceedings of the 21st International Workshop on Mobile Computing Systems and Applications*, 102–102.
- [17] Zhengyou Zhang. 2000. A flexible new technique for camera calibration. *IEEE Transactions on pattern analysis and machine intelligence* 22, 11 (2000), 1330–1334.